Available online at www.sciencedirect.com
SCIENCE DIRECT®
Biochimica et Biophysica Acta 1608 (2004) 11–22
BIOCHIMICA ET BIOPHYSICA ACTA
BBA
www.bba-direct.com

Disruption of a specific molecular interaction with a bound lipid affects the thermal stability of the purple bacterial reaction centre☆

Paul K. Fyfe[a], Neil W. Isaacs[b], Richard J. Cogdell[c], Michael R. Jones[a,*]

[a] *Department of Biochemistry, School of Medical Sciences, University of Bristol, University Walk, Bristol BS8 1TD, UK*
[b] *Department of Chemistry, University of Glasgow, Glasgow G12 8QQ, UK*
[c] *Division of Biochemistry and Molecular Biology, University of Glasgow, Glasgow G12 8QQ, UK*

Received 25 June 2003; received in revised form 16 September 2003; accepted 26 September 2003

Abstract

Relatively little is known about the functions of specific molecular interactions between membrane proteins and membrane lipids. The structural and functional consequences of disrupting a previously identified interaction between a molecule of the diacidic lipid cardiolipin and the purple bacterial reaction centre were examined. Mutagenesis of a highly conserved arginine (M267) that is responsible for binding the head-group of the cardiolipin (to leucine) did not affect the rate of photosynthetic growth, the functional properties of the reaction centre, or the X-ray crystal structure of the complex (determined to a resolution of 2.8 Å). However, the thermal stability of the protein was compromised by this mutation, part of the reaction centre population showing an approximately 5 °C decrease in melting temperature in response to the arginine to leucine mutation. The crystallised mutant reaction centre also no longer bound detectable amounts of cardiolipin at this site. Taken together, these observations suggest that this particular protein–lipid interaction contributes to the thermal stability of the complex, at least when in detergent micelles. These findings are discussed in the light of proposals concerning the unfolding processes that occur when membrane proteins are heated, and we propose that one function of the cardiolipin is to stabilise the interaction between adjacent membrane-spanning α-helices in a region where there are no direct protein–protein interactions.

Keywords: Membrane protein; Membrane lipid; Purple bacterial reaction centre

1. Introduction

Integral membrane proteins inhabit a heterogeneous environment that consists of lipid, water, numerous small molecules and solutes, and other proteins. The amphipathic nature of integral membrane proteins, necessary for these proteins to exist in such a complex environment, means that their purification and crystallisation presents significant technical challenges. Consequently, relatively little high-resolution crystallographic information is available for integral membrane proteins as a group, and there is even less high-resolution structural information on the interactions between these proteins and the surrounding lipids, although new information is now becoming available (see Refs. [1,2] for recent reviews). This is an area of considerable interest, as a huge amount of biochemical and biophysical data has revealed the great importance of protein–lipid interactions for the assembly, stability and function of membrane proteins [2]. However, the lack of detailed structural information has meant that it has been difficult to analyse the significance of individual protein–lipid interactions. A small number of the X-ray crystal structures of integral membrane proteins that are available in the Protein Data Bank (PDB) now contain modelled lipids [1,2], and are presenting the first opportunities to probe the significance of specific protein–lipid interactions through directed mutagenesis (see Ref. [3] for a recent example).

In previous work from our laboratories, an X-ray crystal structure of a single-site mutant of the reaction centre from the purple bacterium *Rhodobacter* (*Rb.*) *sphaeroides* was described, at a resolution of 2.1 Å (PDB entry 1QOV [4]).

Abbreviations: DSC, differential scanning calorimetry; PDB, protein data bank; *Rb.*, *Rhodobacter*

☆ Data deposition: the atomic coordinates and structure factors of the RM267L reaction centre have been deposited in the Protein Data Bank (www.rcsb.org) under code 1UMX.

* Corresponding author. Tel.: +44-117-928-7571; fax: +44-117-928-8274.
E-mail address: m.r.jones@bristol.ac.uk (M.R. Jones).

0005-2728/$ - see front matter © 2003 Elsevier B.V. All rights reserved.
doi:10.1016/j.bbabio.2003.09.014

A large region of continuous density was observed in the electron density map for this reaction centre, located on the intra-membrane surface of the protein. This density was attributed to a single molecule of the diacidic phospholipid diphosphatidyl glycerol, or cardiolipin (Fig. 1A). This electron density feature is also evident in crystallographic data for other mutant reaction centres and the wild-type complex [5–10], and therefore is not present as a consequence of any particular mutation. However, as discussed recently, the quality of the electron density for this lipid is somewhat variable, which may in part be due to sub-stoichiometric binding of the lipid to the detergent-purified reaction centre [9]. Assignment of this electron density feature as cardiolipin was helped by the very distinctive shape of this particular lipid, and has been supported by recent lipid analyses of purified *Rb. sphaeroides* reaction centres that confirm the presence of cardiolipin [7]. Other major lipids associated with the purified *Rb. sphaeroides* reaction centre included phosphatidylcholine, phosphatidylethanolamine and a glycolipid [7]. Camara-Artigas et al. [7] have recently modelled two further lipids, a phosphatidylcholine located on the surface of the M-polypeptide at the cytoplasmic side of the membrane, close to the entrance to the binding pocket of the Q_B ubiquinone, and a glucosylgalactosyl diacylglycerol, also located on the cytoplasmic side of the membrane, close to the membrane-spanning α-helix of the H-polypeptide.

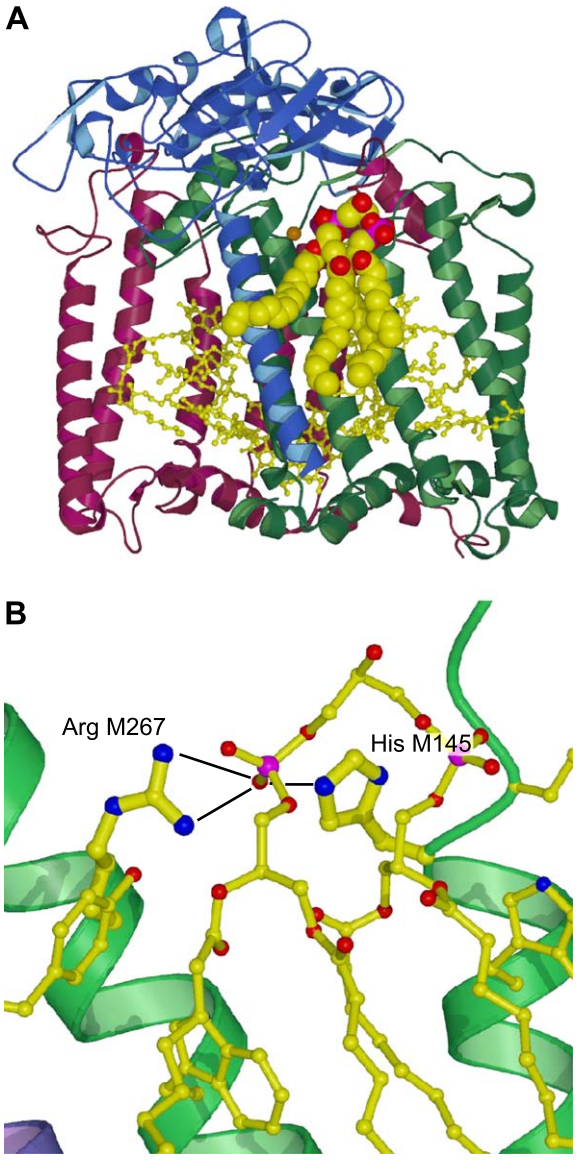

Fig. 1. Molecular structures. (A) The *Rb. sphaeroides* AM260W mutant reaction centre. The L- and M-polypeptides each have five membrane-spanning α-helices (maroon and green, respectively). The H-polypeptide (blue) caps the cytoplasmic faces of the L- and M-polypeptides and has a single membrane-spanning α-helix. The protein encases seven resolved cofactors (yellow ball-and-stick format) and a non-heme iron (brown sphere). The bound cardiolipin in shown in spacefill, in cpk colours. (B) Direct bonding interactions between the P_A phosphoryl of the cardiolipin head-group and residues Arg M267 and His M145. Carbon atoms are shown in yellow, nitrogen in blue, oxygen in red and phosphorus in pink. The green ribbons show the D (left) and C (right) membrane-spanning helices of the M-polypeptide.

Protein sequence alignments show that the residues that bind cardiolipin to the surface of the purple bacterial reaction centre are highly conserved across a range of bacterial species with this type of reaction centre [11]. However, the role, if any, of this particular protein–cardiolipin interaction is not known. To examine this further, in the present work the consequences of disrupting this particular protein–lipid interaction have been examined. Two highly conserved basic residues in the M-polypeptide of the reaction centre that provide the main direct bonding interactions between the protein and the head-group of the bound cardiolipin, His M145 and Arg M267 (Fig. 1B), were changed to Phe and Leu, respectively, by site-directed mutagenesis. The effects of mutation on the binding of cardiolipin were investigated by X-ray crystallography, and their effects on the thermal stability of the reaction centre were examined using Differential Scanning Calorimetry (DSC). The findings of this study are discussed with reference to proposals concerning the unfolding processes that occur when integral membrane proteins are thermally denatured, and a role for cardiolipin in stabilising helix–helix interactions in the reaction centre is proposed.

2. Materials and methods

2.1. Mutagenesis, bacterial growth and reaction centre purification

The mutations Arg M267 to Leu (RM267L) and His M145 to Phe (HM145F) were introduced using procedures described previously [12]. Transconjugant strains with $RC^{+}LH1^{+}LH2^{+}$, $RC^{+}LH1^{+}LH2^{-}$ and $RC^{+}LH1^{-}LH2^{-}$ phenotypes were constructed using the genetic system described previously [13,14].

Details of the growth of the mutant bacterial strains under dark/semiaerobic conditions, and the breakage of harvested cells, are given elsewhere [15]. Membranes for spectroscopic studies were isolated by ultracentrifugation using a sucrose step gradient [15], and membranes for reaction centre purification were pelleted by ultracentrifugation [16]. Reaction centres were purified as described in detail previously [16], and the purity of the reaction centre at each step was assessed by absorbance spectroscopy (see text for details).

2.2. Reaction centre crystallisation and data analysis

The method used for growing trigonal crystals of the RM267L mutant reaction centre was based on that described previously [16,17]. Crystals with space group $P3_121$, were grown by sitting drop vapour diffusion from droplets containing 9 mg/ml reaction centre, 0.09% v/v lauryldimethylamine oxide (LDAO), 3.5% w/v 1,2,3-heptanetriol, 0.75 M potassium phosphate (pH 7.5). The drops were equilibrated against a reservoir of 1.5 M potassium phosphate. Trigonal crystals appeared within 1–4 weeks and grew as prisms of variable size. The crystals had unit cell dimensions of a=b=141.6 Å, c=187.4 Å, α=β=90°, γ=120°.

X-ray diffraction data were collected at room temperature on a 165 mm MAR CCD detector on station 9.5 of the Daresbury Synchrotron Facility. The data were processed using Denzo and Scalepack [18]. Collection and refinement statistics are given in Table 1. Rigid body refinement was performed using REFMAC5 [19] using the coordinates of the wild-type reaction centre [16] as a starting model. This was followed by restrained maximum likelihood refinement in REFMAC5 [19]. In the figures, structures were illustrated using the programs Molscript [20], Raster3D [21] and Xtalview [22].

2.3. Spectroscopy and calorimetry

Absorption spectra of antenna-deficient membranes were obtained using a Beckman DU640 spectrophotometer. To ensure full reduction of the reaction centre primary donor, sodium ascorbate and phenazine methosulfate were added to final concentrations of 1 mM and 25 μM, respectively.

DSC was performed on reaction centre complexes purified to crystallography grade. Experiments were carried out at the BBSRC/EPSRC Biological Microcalorimetry Facility (University of Glasgow) using a MicroCal Instruments VP-DSC with a 0.5 ml sample cell. Scans were taken using 0.25 mg/ml protein in 20 mM Tris–HCl (pH 8.0), 0.1% LDAO, scanning from 10 to 80 °C at a scan rate of 90 °C/h. The heat capacity was measured as a function of temperature (°C), and was converted to the molar heat capacity, C_p (kJ mol^{-1} K^{-1}), by accounting for the sample concentration and cell volume. A baseline correction was performed by subtracting the result of a buffer versus buffer scan under identical conditions. The area under the DSC curve corresponds to the molar enthalpy change for the phase transition, ΔH_{cal} (kJ mol^{-1}).

Table 1
Crystallographic statistics for data collection and refinement

	RM267L reaction centre
Collection statistics	
Number of unique reflections	50,050
Completeness (%)[a]	97.5 (92.2)
Multiplicity	2.5
R_{merge} (%)[a,b]	6.2 (44.0)
Refinement statistics	
Resolution range (Å)	29–2.8
R factor (%)[c]	22.3
R_{free} (%)[d]	24.8
Average B factor (Å^2)	44.1
Geometry	
RMSD from ideality	
Bonds (Å)	0.021
Angles (°)	2.4
Residues in the Ramachandran plot (%)[e]	
Most favoured regions	88.2
Additional allowed areas	11.0
Generously allowed areas	0.7
Disallowed areas	0.0
Coordinate error (Å)[f]	0.36
Model	
Number of protein residues	823
Number of cofactors	4 bacteriochlorophyll 2 bacteriopheophytin 1 ubiquinone 1 spheroidenone 1 iron atom
Number of waters	16
Number of detergents	2 LDAO
Number of phosphates	1

[a] Figures within brackets refer to the statistics for the outer resolution shell (2.9–2.8 Å).

[b] $R_{merge}=\Sigma_h\Sigma_i|<I(h)>-I(h)_i|/\Sigma_h\Sigma_i I(h)_i$ where $I(h)$ is the intensity of reflection h, Σ_h is the sum over all reflections, Σ_i is the sum over all i measurements of reflection h.

[c] R-factor is defined by $\Sigma|F_O|-|F_C|/\Sigma|F_O|$.

[d] Free-R was calculated with 5% reflections [52] selected to be the same as in the wild-type RC refinement [16].

[e] Ramachandran plot was produced by Procheck version 3.0 [53].

[f] Coordinate error was estimated by Cruickshank's DPI [54].

3. Results and discussion

3.1. Construction and characterisation of the mutant reaction centres

X-ray crystal structures of the *Rb. sphaeroides* reaction centre show that, in addition to a number of indirect contacts mediated by water molecules, the polar head-group of cardiolipin makes direct contacts with the side-chains of amino acids Arg M267 and His M145 (Fig. 1B), and with the

backbone amide of Lys M144 [4]. To investigate the effects of disrupting this membrane protein–lipid interaction, residues Arg M267 and His M145 were separately mutated to Leu and Phe, respectively (see Materials and methods). The mutated reaction centre genes were expressed in strains of *Rb. sphaeroides* in which the reaction centre is the sole pigment–protein complex, and strains that also contain either just the LH1 antenna complex or both the LH1 and LH2 antenna complexes (see Materials and methods).

Absorbance spectroscopy of intact cells and isolated photosynthetic membranes showed that the expression level of the reaction centre was not affected by either mutation. To illustrate this, Fig. 2a shows spectra of photosynthetic membranes prepared from strains that have the reaction centre and the LH1 antenna complex, but lack the LH2 antenna. In wild-type strains, the reaction centre and the surrounding LH1 antenna have a fixed stoichiometry, even though both complexes are capable of being expressed independently from one another. The relative level of reaction centre expression can therefore be assessed by comparing the amplitude of the absorbance band at 875 nm, which is mainly attributable to the bacteriochlorophylls of the LH1 antenna complex, with the amplitude of the absorbance band at 805 nm, which is attributable to the bacteriochlorophylls of the reaction centre. The relative amount of the reaction centre is known to decrease in response to mutations that affect assembly or stability of the complex (unpublished observations). In the present study, neither mutation affected the amplitude of the 805 nm band relative to the LH1 absorbance band at 875 nm, demonstrating that the relative amounts of reaction centre and LH1 antenna were normal.

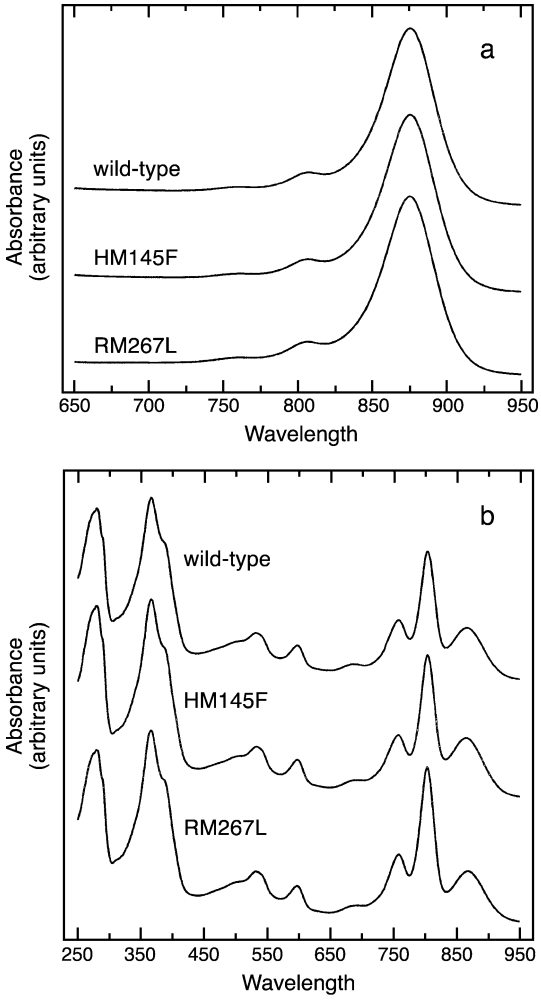

Fig. 2. (a) Absorbance spectra of intracytoplasmic membranes containing the LH1 antenna and wild-type, HM145F or RM267L reaction centres. (b) Absorbance spectra of purified reaction centres, recorded immediately prior to crystallisation.

Absorbance spectra of photosynthetic membranes prepared from strains that had the reaction centre as the sole pigment–protein complex showed that neither mutation had a major effect on the absorbance spectrum of the four bacteriochlorophylls and two bacteriopheophytin cofactors of the reaction centre (data not shown). Extensive studies have shown that the absorbance properties of these cofactors are very sensitive to changes in the structure of the protein–cofactor matrix, and so this result provided good evidence that neither mutation had a significant effect on the overall structure of the reaction centre. In the case of the RM267L reaction centre, there was a small decrease in the relative intensity of the absorbance band at 867 nm, attributable to the "special pair" of primary donor bacteriochlorophylls (see below). This small change was also seen for purified reaction centres (Fig. 2b).

Experiments carried out on strains that had the reaction centre and both the LH1 and LH2 antenna complexes showed that neither mutation affected the capacity of the reaction centre to support photosynthetic growth, either on solid media incubated in an illuminated anaerobic growth chamber, or in filled bottles of liquid media incubated in an illuminated water bath. The rate of photosynthetic growth under these conditions was not influenced by either mutation (data not shown).

3.2. Purification of the mutant reaction centres

Having established that the mutations had no radical effects on the structure or function of the reaction centre, the mutant complexes were purified with a view to conducting crystallisation trials. During the purification it became apparent that the RM267L mutation had affected the ease with which the reaction centre could be purified, and the purity of the final product. A convenient aspect of the biochemistry of the reaction centre is that the purity of the complex can be assessed by absorbance spectroscopy, measuring the ratio of protein absorbance at 280 nm to bacteriochlorophyll absorbance at 802 nm (A^{280}/A^{802}) [23]. When the value of A^{280}/A^{802} falls below 1.3, the reaction centre is sufficiently pure for crystallisation.

The absorbance spectra of wild-type, HM145F and RM267L reaction centres prepared for crystallisation are

shown in Fig. 2b. As in previous studies, purification of a sufficient quantity of wild-type and HM145F reaction centres required the use of three anion exchange columns followed by a preparative gel filtration column [16]. The final product showed the usual A^{280}/A^{802} of ~1.3 (Fig. 2b). In contrast, purification of the RM267L mutant required only two anion exchange purification steps to approach the A^{280}/A^{802} ratio of 1.3. The spectrum of the final, purified RM267L reaction centres is also shown in Fig. 2b. Unusually, the final value of A^{280}/A^{802} was 1.1 for this mutant. Our interpretation of this result is that the RM267L mutation lessens the tendency of the reaction centre to associate with other proteins during purification, and so the preparation of highly pure reaction centres is more easily achieved. The identity of these proteins, and any possible functional significance of this observation, are the subject of an ongoing investigation.

3.3. Crystallisation of the mutant reaction centres

The purified mutant reaction centres were crystallised, using the procedure described in Materials and methods. Crystals of the HM145F mutant complex displayed the same morphology as crystals obtained in previous studies for the wild-type reaction centre [16,17], exhibiting a hexagonal cross-section with a length of 0.5–1.0 mm. However, although crystals of the RM267L reaction centre were of the same form, they were unusually large, with lengths of up to 2.0 mm and a cross-section of up to 0.75 mm. Further structural studies of the HM145F mutant reaction centre were not pursued, but diffraction data were collected at room temperature using one crystal of the RM267L mutant, over the resolution range 28.0–2.8 Å. The unusual length of these RM267L crystals allowed the crystal to be translated three times during data collection, in order to minimise the effects of radiation damage. Data processing and refinement of the structural model were carried out as described in Materials and methods, and the relevant statistics are given in Table 1.

3.4. The structural model of the RM267L reaction centre

The final structural model of the RM267L reaction centre was comprised of residues 1–281 of the L-polypeptide, residues 1–302 of the M-polypeptide and residues 11–250 of the H-polypeptide. Amino acids 303–307 of the M-polypeptide and 1–10 and 251–260 of the H-polypeptide were not included due to the absence of corresponding electron density. Also included in the model were four molecules of bacteriochlorophyll, two molecules of bacteriopheophytin, one non-heme iron atom, one molecule of spheroidenone and the Q_A ubiquinone. Insufficient density was observed in the Q_B binding pocket to allow modelling of this cofactor. The Q_B ubiquinone is able to freely dissociate from the complex, and hence the occupancy of this site is generally low in purified complexes. Finally, 16 water molecules and two molecules of the detergent LDAO were also modelled.

Residue arginine M267 is located on the intra-membrane surface of the reaction centre (Fig. 1A), and the electron density map in the region of this residue was consistent with the replacement of this arginine by a leucine. Examination of the overall structural model of the RM267L reaction centre, and comparison with that of the wild-type complex, showed that the replacement of the arginine with a leucine had no discernable effect on the structure of the protein–cofactor complex, within the limits imposed by the resolution of the data, other than truncation of the M267 side-chain. This is in accord with the spectroscopic data and growth studies, which imply that the mutation does not affect the structural or functional integrity of the reaction centre. The structural basis for the slightly less intense 865 nm absorbance band was not apparent, but it is known that the characteristics of this absorbance band are extremely sensitive to the detailed geometry of the primary donor bacteriochlorophylls and the surrounding protein.

3.5. Interpretation of electron density in the region usually occupied by cardiolipin

Fig. 3 shows the 2 mF_o-DF_c electron density map in the region occupied by cardiolipin in (A) the AM260W reaction centre [4], (B) a reaction centre with the mutations GM203D and FM197R [24] and (C) the RM267L reaction centre. Density not attributable to the protein is highlighted in green. The GM203D/FM197R reaction centre is included for comparison as its structure was based on diffraction data of similar resolution and quality to that of the RM267L model. Briefly, the GM203D/FM197R structure was determined from data collected over the range 29–2.8 Å, with a completeness of 92.6%. The refined model had an *R* factor of 22.3%, and a *R*-free value of 24.8% [24]. These statistics are similar to those for the data on the RM267L reaction centre given in Table 1.

The molecule of cardiolipin is clearly resolved as a continuous electron density feature in the data for the AM260W reaction centre (Fig. 3A) and gives rise to a less complete feature in the electron density map for the GM203D/FM197R reaction centre (Fig. 3B). In some of the other data sets produced by our laboratories for the wild-type or mutant reaction centres, density features in this region have been found that correspond to fragments of this cardiolipin, but were insufficiently complete for the lipid to be included in the final structural model, whilst in other data sets, a complete electron density feature was resolved. A detailed discussion of this variability, including representative electron diffraction data, has been published recently [9].

The reason for the variability in the quality of the electron density corresponding to the cardiolipin in different structures has not yet been determined, although it probably reflects the occupancy of the cardiolipin binding site in

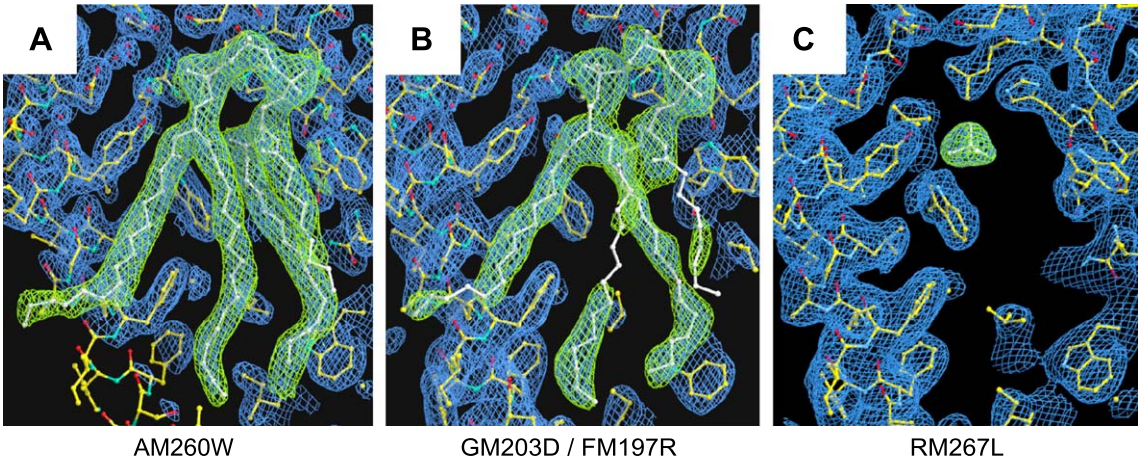

Fig. 3. Electron density at the surface of the reaction centre. (A) REFMAC 2 mF_o-DF_c electron density map (blue) for the AM260W reaction centre, contoured at 1.0 σ, with the fitted structure of the protein (in cpk colours) and cardiolipin (in white). Overlaid is the electron density attributed to cardiolipin (highlighted in green). (B) The cardiolipin molecule as resolved in data for the FM197R/GM203D reaction centre, shown as for (A). (C) Equivalent view of the 2 mF_o-DF_c electron density map for the RM267L reaction centre. The new electron density feature is highlighted in green, and the modelled phosphate is shown in white (see text). The RM267L mutation did not affect the structure of the protein–cofactor system other than the M267 side-chain.

different crystal preparations and the nature of the diffraction data collected [9]. In particular, we have noticed that the structures in which the cardiolipin electron density was most complete was based on diffraction data that included low resolution terms (up to 30 Å). Thus, although the data on the AM260W reaction centre represent the highest resolution data set we have collected to date (2.1 Å), it may be that inclusion of low-resolution data is of more importance for the observation of surface features such as bound lipids. In support of this, Camara-Artigas et al. [7] have recently published a new structure of the wild-type *Rb. sphaeroides* reaction centre that includes three bounds lipids, including the cardiolipin discussed here. This structure was based on diffraction data collected over the range 30–2.55 Å, and so included low-resolution terms. The quality and completeness of the electron density corresponding to the cardiolipin in the data of Camara-Artigas et al. [7] was similar to that shown in Fig. 3A for the AM260W mutant. Along the same theme, the phosphatidylcholine and glycolipid modelled by Camara-Artigas et al. [7] were not included in the structural model of the RM267L reaction centre, as the corresponding electron density was incomplete.

Despite variability in the completeness of the electron density corresponding to the cardiolipin, in all of the (~20) structures for the *Rb. sphaeroides* reaction centre determined to date by our laboratories the density attributable to the P_A phosphoryl of the cardiolipin has always been present, located within bonding distance (~2.8–3.5 Å) of the side-chains of amino acids Arg M267 and His M145. Some elongated density in a position equivalent to the most deeply buried acyl chain of the cardiolipin is also almost always resolved (tail 4, second chain from the right in Fig. 3A). This is presumably because these are the regions of the cardiolipin that are subject to the greatest motional restriction by the adjacent protein surface.

In the case of the RM267L reaction centre, the pattern of non-protein electron density features in this region were different from that in any of our previous structures (Fig. 3C). The maps calculated for the RM267L reaction centre lacked any electron density that could correspond to the P_A phosphoryl group or any of the acyl tails of the cardiolipin molecule. However, a strong peak of density (3 σ) was found in a position approximately 4 Å lower in the membrane, and 2 Å deeper into the groove on the protein surface, than that usually occupied by the P_A phosphoryl. The density peak was too intense to be a water molecule, and had a tetrahedral form suggesting that it had arisen from a complex ion such as phosphate. A phosphate molecule was therefore modelled into this electron density feature. In the final structural model, this phosphate was positioned within bonding distance of the side-chains of Tyr H30 (3.3 Å), Trp M271 (3.1 Å), and His M145 (3.5 Å). In the wild-type and AM260W reaction centres, these amino acids are involved in binding of the P_A phosphoryl group of cardiolipin (Tyr H30 is on the centre, left in Fig. 1B). However, their interactions with the modelled phosphate in the structure of the RM267L reaction centre were markedly different from those observed previously in other reaction centres.

A number of the structures for the purple bacterial reaction centre deposited in the PDB include modelled phosphates or sulfates [25–27], and it is not uncommon to find components of the crystallisation buffers being specifically bound within a crystal. However, another possibility is that this electron density feature represents an ordered part of an otherwise disordered molecule such as a lipid or detergent. As an example, the LDAO detergent used in the crystallisations has a tetrahedral head-group that would fit the observed density. However, there was insufficient electron density available to support the fitting of a detergent tail leading from this region. Our conclusion

therefore is that the altered pattern of electron density in this region suggests that cardiolipin is no longer bound to the protein surface in purified and crystallised reaction centres carrying this arginine to leucine mutation. The surrounding polar groups that usually interact with the cardiolipin headgroup are seen to have formed a new interaction with a molecule that can be modelled as a complex ion (phosphate), although we cannot discount the possibility that this could represent part of a largely disordered detergent or lipid molecule.

3.6. Differential scanning calorimetry

The results of the X-ray crystallography indicate that the reaction centre–cardiolipin interaction is weakened by the RM267L mutation to such an extent that the cardiolipin is no longer resolved in the X-ray structure of the purified complex. To examine whether this apparent disruption of this protein–lipid interaction had any other consequences, DSC was used to examine the thermal stability of the wild-type and mutant reaction centres.

Fig. 4 shows the results of DSC carried out on reaction centres that were purified to the same degree as those used for X-ray crystallography. In the case of the wild-type and HM145F reaction centres, the DSC measurements revealed two overlapping endothermic transitions. For the wild-type complex, a fit of the experimental data with two components yielded denaturation transition temperatures (T_m) of 47.1 and 54.8 °C, with associated calorimetric enthalpies (ΔH_{cal}) of 151.5 and 253.6 kJ mol^{-1}. Analysis of the data for the HM145F complex yielded values of T_m of 48.1 and 55.5 °C for the two transitions, and associated values of ΔH_{cal} of 168.9 and 305.0 kJ mol^{-1}. In contrast, the purified RM267L reaction centres showed only a single transition with a T_m of 50.5 °C and a ΔH_{cal} of 305.4 kJ mol^{-1}.

What could be the explanation for the biphasic behaviour of the wild-type and HM145F complexes, and the monophasic behaviour of the RM267L reaction centre? In previous DSC studies of integral membrane proteins, two component traces have been observed in cases where thermal denaturation involves the unfolding of distinct protein domains. An example is the FhuA outer membrane protein from *Escherichia coli*, that has a two-domain structure consisting of a 22-strand β-barrel that forms a transmembrane channel, and a globular domain that forms a "cork" located within the channel [28]. DSC of this iron chelate transporter yielded two transitions centred at 65 and 75 °C, that were attributed to unfolding of the cork and barrel domains, respectively [28]. Likewise, cytochrome oxidase exhibited two distinct transitions that were assigned to unfolding of subunit III at lower temperatures, and a subunit I/II core domain at higher temperatures [29]. Given this, one possible explanation of the behaviour of the wild-type and HL145F complexes in the present study is that unfolding of the reaction centre involves two domain-unfolding processes with values of T_m that differ by 7–8 °C. However, if this explanation is correct, then this implies that the RM267L mutation affects the stability of the more thermally tolerant unfolding domain, such that unfolding of the RM267L protein appears to involve a single process. The results of X-ray crystallography argue against this, as the RM267L mutation has no discernable effect on the structure of the reaction centre protein other than the change in side-chain structure of the M267 residue itself.

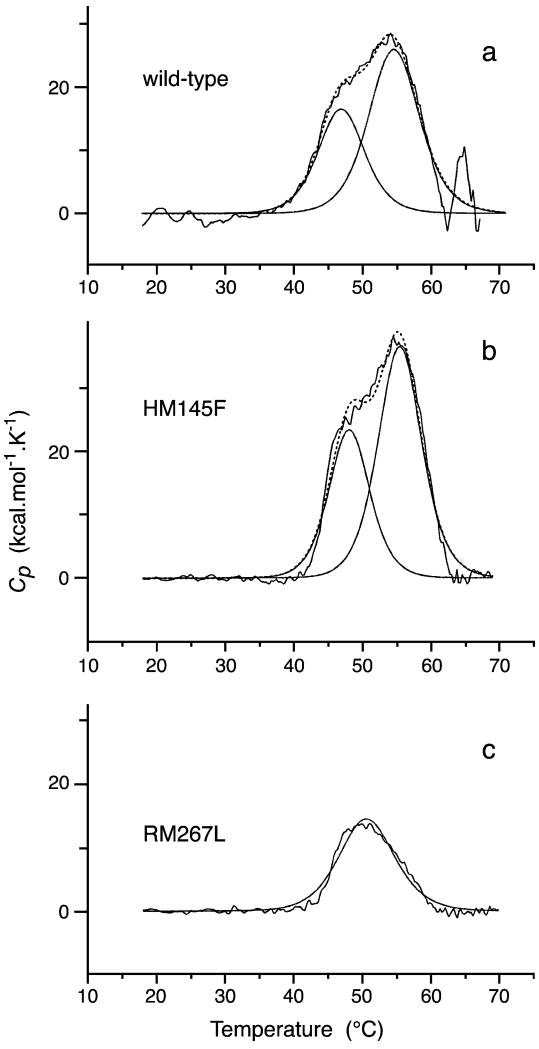

Fig. 4. DSC profile for purified (a) wild-type reaction centres, (b) HM145F reaction centres and (c) RM267L reaction centres. In (a) and (b), continuous lines show the best theoretical fit for two independent components, obtained by deconvolution of the original scan.

Another possibility is that the two transitions observed in the DSC experiment arise from different aggregation states of the reaction centre. As an illustration, Zhou and Bowie [30] have recently shown that mutations that increase the thermal stability of the integral membrane protein diacylglycerol kinase also enhanced the stability of the trimeric form of the complex relative to the monomeric form. Having said this, there is no strong evidence that the *Rb. sphaeroides* reaction centre forms dimers or multimers either in the

membrane or when solubilised in detergent. Certainly the crystallised form of the complex is monomeric, and data from electron microscopy on the core complex formed between the reaction centre and the LH1 antenna also suggests that the reaction centre itself is monomeric, although the core complex may be dimeric [31–36].

The remaining possibility is that the two transitions observed in the DSC experiment on the wild-type complex are due to heterogeneity, with two populations of reaction centres that undergo the same unfolding process, but with different values of T_m. At least two possible sources of heterogeneity are provided by the crystallographic data outlined above, which indicate partial occupancy of both the Q_B ubiquinone binding site and the cardiolipin binding site adjacent to the M267 residue. Partial occupancy of the Q_B site by ubiquinone in purified reaction centres is well documented, and leads to poor quality electron density for this cofactor unless the site is reconstituted by adding ubiquinone. However, partial occupancy of the Q_B site is unlikely to be relevant to the DSC results described above, as it affects both the wild-type and mutant reaction centres. In the case of the cardiolipin binding site, partial occupancy of this site has been discussed with reference to the variable quality and completeness of the electron density attributable to this lipid. In this case, the proposal would be that the higher temperature transition is attributable to a population of reaction centres that are stabilised due to the binding of a cardiolipin.

The size of this stabilisation, some 7–8 °C, is consistent with the magnitude of effects observed in DSC experiments on adding lipids to membrane proteins, or removing them through phospholipase action. For example, delipidation of purified cytochrome oxidase produces a 5 °C decrease in T_m for this complex [37]. The addition of cholesterol to cardiac microsomes containing Ca^{2+}/Mg^{2+}ATPase increased the T_m of the transition assigned to this membrane protein by 2 °C [38]. The stabilising influence of the phospholipid environment of integral membrane proteins has been shown through studies of the band 3 anion transporter of erythrocytes reconstituted into artificial bilayers, where T_m was observed to vary with acyl chain length (3–5 °C per two carbon units), unsaturation (3–5 °C per double bond) and head-group type (~18 °C difference between uncharged and charged lipids) [39]. The presence of cofactors or the application of treatments that interrupt the continuity of the protein backbone have also been shown to have an influence on the thermal stability of integral membrane proteins. In the case of bacteriorhodopsin, removal of the retinal cofactor bound at the centre of the complex has been observed to induce a 16 °C decrease in T_m in DSC experiments on membrane-bound complexes [40]. Destabilising the structural integrity of bacteriorhodopsin by introducing a single bond cut between helices B and C decreased T_m by 6 °C [40]. In summary then, the size of the destabilising effect of the RM267L mutation seen in the present study is of the same order as that seen when the lipid environment of an integral membrane protein is altered, or when a change is made that destabilises part of the protein structure.

3.7. Interpretation of the effects of the RM267L mutation

Our favoured interpretation of the effects of the RM267L mutation on the thermal stability of the complex is based on two observations. First, the variability in the quality of the electron density attributable to cardiolipin in different reaction centre structures suggests less than 100% occupancy of the binding site by the lipid in the purified form of the complex [9]. Second, the RM267L mutation appears to weaken the binding of cardiolipin to such an extent that it is no longer detectable in the X-ray data (Fig. 3C). Drawing on these observations, we propose that the biphasic response seen in the DSC measurements on the wild-type reaction centre arises from a mixed population of proteins, the ~48 and ~56 °C transitions corresponding to complexes with and without cardiolipin bound at this site. The HM145F mutation, which has no discernable effect on the spectroscopic or biochemical properties of the reaction centre, presumably does not affect the affinity of cardiolipin for this binding site on the reaction centre, and the two-component DSC profile is maintained, albeit with some small variations (≤1 °C) in T_m values. However, the RM267L mutation weakens cardiolipin binding to such an extent that the lipid is no longer bound to the purified form of the complex at the site in question, and the purified RM267L reaction centre exhibits only the lower of the two melting temperatures.

In an attempt to test this hypothesis, DSC traces were recorded for wild-type reaction centres in the presence of added cardiolipin. This treatment produced a narrower DSC trace, indicating less sample heterogeneity, and a shift in favour of a slightly higher T_m value (~2 °C; data not shown). However, these results were difficult to reproduce and so were rather inconclusive. An attempt to deplete wild-type reaction centres of cardiolipin, through addition of phospholipase A2, led to breakdown of the sample. An additional complicating feature of these biochemical treatments is that they open up the possibility of effects arising from non-specific reactions, such as binding of cardiolipin to other sites on the protein surface or the digestion of other lipids by the phospholipase, and so even if a reproducible effect was to be seen in such experiments, it would be difficult to attribute this to the specific protein–lipid interaction under examination.

Finally, we turn to the question of why mutation of Arg M267 affects the properties of the reaction centre in the ways described, but mutation of His M145 does not produce effects of an equal magnitude. The answer may lie in the extent of the bonding interaction between each side-chain and the adjacent cardiolipin head-group. In the case of His M145, binding appears to involve a single hydrogen bond between the NE2 nitrogen of the His side-chain and the OA3 oxygen of the P_A phosphoryl group of the cardiolipin

(Fig. 5A). In the case of the Arg M267 residue, a more extensive interaction can be traced (Fig. 5A). Both terminal −NH groups are within hydrogen bonding distance of the cardiolipin OA3 oxygen of the P_A phosphoryl group (2.8 and 3.2 Å), and one of these −NH groups is also within hydrogen bond distance of a crystallographically defined water. This water, in turn, is within hydrogen bond distance of the OA7 carbonyl oxygen at the top of acyl chain 1, and the OB9 carbonyl oxygen at the top of acyl chain 4. Thus it seems feasible that the loss of a single hydrogen bond donated by His M145 would not weaken binding of the cardiolipin head-group to the same extent as loss of the network of interactions involving Arg M267.

3.8. The role of the cardiolipin bound to the purple bacterial reaction centre

It has been established that proteins such as the bacterial reaction centre preferentially interact with anionic lipids such as cardiolipin [41,42], but to our knowledge there has been no specific study of the effect of cardiolipin on the structural and functional properties of the bacterial reaction centre. However, it is known that cardiolipin is important for the maintenance of optimal activity of a number of major integral membrane proteins, particularly in mitochondria [43,44].

Recently, the role of a crystallographically defined cardiolipin molecule bound to the cytochrome bc_1 complex from yeast has been investigated by mutagenesis of three lysine residues that bind the head-group of this lipid [3]. Although single mutations had no discernable effect on cytochrome bc_1 activity, double and triple combinations of mutations led to lowered levels of this complex, indicating an important role for the lipid in maintaining the stability of the complex, or in its assembly. Lange et al. [3] also pointed out that the cardiolipin is located close to a hydrogen bond network that connects the ubiquinone reductase (Q_i) site to the surface of the cytochrome bc_1 complex. This network (or proton wire) has been implicated in the delivery of protons from the aqueous phase to the Q_i site, where ubiquinone is doubly reduced and doubly protonated, forming ubiquinol. The location of the cardiolipin at the entrance of this proton delivery pathway suggests a role for the lipid as a proton reservoir [3]. In principle, a similar role could be

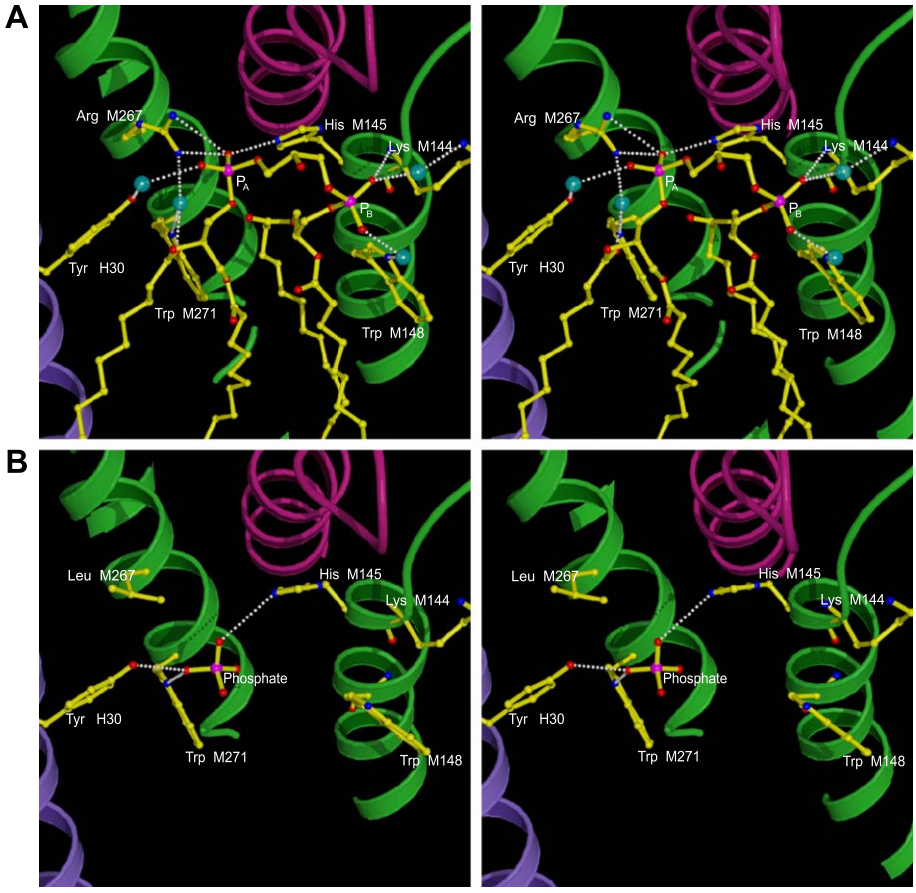

Fig. 5. (A) Stereo view of the bonding interactions between the cardiolipin head-group and the surrounding protein, as revealed in the structural model of the AM260W reaction centre. Cardiolipin and the bonded amino acid residues are shown in stick format (cpk colours), and crystallographically defined waters are shown as blue spheres. The cardiolipin connects the D and E membrane-spanning helices of the M-polypeptide (green ribbons, left and right, respectively) at the point where they are separated by the C membrane-spanning helix of the L-polypeptide (magenta ribbon, top centre). (B) Stereo view of the equivalent region of the protein in the structural model of the RM267L reaction centre. Colour coding is as for Fig. 1.

considered for the cardiolipin bound to the *Rb. sphaeroides* reaction centre, as this complex also has a ubiquinone reductase site (Q_B) that connects to the extra-membrane surface of the protein via hydrogen bond networks [45,46]. However, this cardiolipin is located some 15 Å from the Q_B site, and is remote from the hydrogen bond networks that are proposed to connect the Q_B site to the aqueous phase, and therefore a role for this lipid as a local proton buffer seems unlikely.

In the *Rhodopseudomonas viridis* reaction centre, the Arg residue that is structurally equivalent to Arg M267 in *Rb. sphaeroides* has been proposed to form part of a cluster of 24 residues that are electrostatically coupled to the Q_A ubiquinone [47]. Consistent with this proposal, mutagenesis of the adjacent residue Ile M265 has been shown to alter the mid-point redox potential of the Q_A/Q_A^- couple [48], indicating that the detailed structure of this part of the reaction centre does indeed have an influence on the redox properties of the Q_A ubiquinone. Intriguingly, it has also recently been reported that addition of cardiolipin to isolated reaction centres lowers the mid-point potential of Q_A/Q_A^- by 30–40 mV, bringing it closer to the value seen in membrane-bound reaction centres [49]. However, recent data has shown that this effect is not influenced by the RM267L mutation reported here [49], and so it is not clear whether this effect of cardiolipin is related to the binding site that is the subject of the present study, or other reaction centre–cardiolipin interaction(s) that remain to be characterised.

Analysis of the extensive sequence information now available for purple bacterial reaction centres indicates that the residues that interact with the head-group of the cardiolipin in the *Rb. sphaeroides* reaction centre are highly conserved [11]. This suggests that, whatever its role, this particular protein–lipid interaction is a conserved structural feature of all purple bacterial reaction centres (with the caveat that, as discussed elsewhere [11], it is not established that all purple photosynthetic bacteria contain cardiolipin as a component of the cytoplasmic membrane). In our previous reports, we have speculated on the possible role of this bound lipid, including the possibility that it forms part of a contact surface between the reaction centre and other proteins, or perhaps between reaction centres in a dimer [4,11]. Some support for such a role comes from the observation that the behaviour of the reaction centre during purification is altered when the cardiolipin binding site is perturbed by the RM267L mutation, and we are currently investigating this further.

In a very recent report, Katona et al. [50] have described a new crystal form of the *Rb. sphaeroides* reaction centre, grown from protein embedded in a lipid cubic phase. The structure of the reaction centre was determined from these crystals to a resolution of 2.35 Å, and the structural model included the cardiolipin discussed in the present report. This new 3D crystal takes the form of stacked 2D crystals, with all reaction centres having the same orientation within each layer, and the internal two-fold symmetry axis of each reaction centre making an angle of 11.5° with respect to the short axis of the 2D crystal. Within each layer, the reaction centres are therefore arranged approximately as they would be in a lipid bilayer. Within the crystal, alternate layers have opposite orientations, such that inter-layer crystal contacts alternate between the cytoplasmic region of the H-polypeptide, and contacts between the periplasmic regions of the L-/M-polypeptides. Intriguingly, from the point of view of the present report, within the individual planes the orientated reaction centres appear to be arranged in pairs around an axis of two-fold symmetry. The contact surface between the two reaction centres consists of intra-membrane regions of the M- and H-polypeptides, and includes the cardiolipin binding site described above. In this new crystal form, the molecular contacts between the reaction centre and the bound cardiolipin described by us previously are preserved, with prominent roles played by Arg M267, His M145 and Lys M144 [4,50], but there is also a new contact between the P_B phosphoryl of the cardiolipin (on the right in Figs. 1B and 5) and residue Lys L202 of the symmetry-related reaction centre [50]. This new crystallographic data thus gives an interesting insight into how the cardiolipin could facilitate molecular contacts in a dimer of reaction centres, although the question of whether the *Rb. sphaeroides* reaction centre forms dimers in the native photosynthetic membrane is still an open question.

The main outcome of the present study is the suggestion that the bound cardiolipin contributes to the thermal stability of the purified form of the reaction centre. In seeking to understand this, it is helpful to consider the processes involved in the thermal unfolding of integral membrane proteins. A recurring theme that has emerged from DSC studies is that the enthalpy change that occurs on unfolding of a membrane protein is smaller than the typical changes observed for the unfolding of water-soluble proteins of similar molecular weights (see Ref. [29] for a review). This has been taken as evidence that overall unfolding of a membrane protein does not involve the unfolding of the membrane-spanning α-helices, a conclusion supported by CD spectroscopy. Rather, it has been proposed that this enthalpy change mainly reflects loss of secondary and tertiary structure in extra-membrane domains, including loops that connect membrane-spanning helices, and perhaps the loss of packing interactions between membrane-spanning α-helices [29,51].

The view that thermal denaturation of membrane proteins involves unfolding of protein elements that connect the α-helices provides a possible structural role for the cardiolipin that is bound to the *Rb. sphaeroides* reaction centre. As can be seen in Fig. 5A, the head-group of this lipid is bound to residues located at the cytoplasmic ends of α-helices D and C of the M-polypeptide (green ribbons). At the periplasmic side of the membrane, these α-helices are in van der Waals' contact with one another, but in the region that binds the head-group of the cardiolipin on the opposite side of the membrane, these helices splay apart due to interdigitation

with the E α-helix of the L-polypeptide (Fig. 5A, maroon ribbon). The extended head-group of the cardiolipin binds to residues in both M-polypeptide α-helices, at a level in the membrane where there are no direct interactions between the two. Immediately above the cardiolipin binding site the E α-helix of the L-polypeptide projects between the D and C α-helices of the M-polypeptide, and forms an overhang below which the cardiolipin binds.

The cross-contacts between the D and C α-helices of the L-polypeptide provided by the cardiolipin are traced in Fig. 5A. The P_A phosphoryl makes extensive contacts with residues on the D-helix of the M-polypeptide, as well as with His M145 on the C-helix (and Tyr H30 on the single membrane-spanning helix of the H-polypeptide). The P_A phosphoryl is covalently bonded to the P_B phosphoryl, which in turn has extensive interactions with residues on the C-helix of the M-polypeptide. As can be seen from the X-ray crystal structure of the RM267L mutant (Fig. 5B), one consequence of the loss of the cardiolipin is that the cross-bracing between these helices involving multiple covalent and hydrogen bonds is replaced by a single hydrogen bond interaction mediated by the molecule we have assigned as a phosphate. Thus a possible structural role for the cardiolipin could be to stabilise this part of the underlying protein structure, a stabilising influence that is compromised when Arg M267 is mutated to Leu, but not when His M145 is mutated to Phe. As discussed above, a further role could be to form part of the monomer–monomer contact surface in a reaction centre dimer, as recently visualised in the crystallographic data of Katona et al., although the in vivo relevance of such a dimeric *Rb. sphaeroides* reaction centre remains to be proven.

Acknowledgements

The authors wish to thank Professor Alan Cooper and Margaret Nutley at the BBSRC/EPSRC Biological Microcalorimetry Facility, University of Glasgow for guidance and assistance with the DSC measurements. We also thank the staff at beamline 9.5 of the Daresbury Synchrotron Radiation Source for their assistance with data collection. This work was funded by the Biotechnology and Biological Sciences Research Council of the United Kingdom.

References

[1] P.K. Fyfe, K.E. McAuley, A.W. Roszak, N.W. Isaacs, R.J. Cogdell, M.R. Jones, Probing the interface between membrane proteins and membrane lipids by X-ray crystallography, Trends Biochem. Sci. 26 (2001) 106–112.

[2] A.G. Lee, Lipid–protein interactions in biological membranes: a structural perspective, Biochim. Biophys. Acta 1612 (2003) 1–40.

[3] C. Lange, J.H. Nett, B.L. Trumpower, C. Hunte, Specific roles of protein–phospholipid interactions in the yeast cytochrome bc_1 complex structure, EMBO J. 20 (2001) 6591–6600.

[4] K.E. McAuley, P.K. Fyfe, J.P. Ridge, N.W. Isaacs, R.J. Cogdell, M.R. Jones, Structural details of an interaction between cardiolipin and an integral membrane protein, Proc. Natl. Acad. Sci. U. S. A. 96 (1999) 14706–14711.

[5] K.E. McAuley, P.K. Fyfe, R.J. Cogdell, N.W. Isaacs, M.R. Jones, X-ray crystal structure of the YM210W mutant reaction center from *Rhodobacter sphaeroides*, FEBS Lett. 467 (2000) 285–290.

[6] A. Camara-Artigas, C.L. Magee, J.C. Williams, J.P. Allen, Individual interactions influence the crystalline order for membrane proteins, Acta Crystallogr., D Biol. Crystallogr. 57 (2001) 1281–1286.

[7] A. Camara-Artigas, D. Brune, J.P. Allen, Interactions between lipids and bacterial reaction centres determined by protein crystallography, Proc. Natl. Acad. Sci. U. S. A. 99 (2002) 11055–11060.

[8] A. Camara-Artigas, C. Magee, A. Goetsch, J.P. Allen, The structure of the heterodimer reaction center from *Rhodobacter sphaeroides* at 2.55 angstrom resolution, Photosynth. Res. 74 (2002) 87–93.

[9] M.R. Jones, P.K. Fyfe, A.W. Roszak, N.W. Isaacs, R.J. Cogdell, Protein–lipid interactions in the bacterial reaction centre, Biochim. Biophys. Acta 1565 (2002) 206–214.

[10] P.R. Pokkuluri, P.D. Laible, Y.L. Deng, T.N. Wong, D.K. Hanson, M. Schiffer, The structure of a mutant photosynthetic reaction center shows unexpected changes in main chain orientations and quinone position, Biochemistry 41 (2002) 5998–6007.

[11] M.C. Wakeham, M.R. Jones, R.B. Sessions, P.K. Fyfe, Is there a conserved interaction between cardiolipin and the Type II bacterial reaction center?, Biophys. J. 80 (2001) 1395–1405.

[12] J.P. Ridge., The role of the protein during energy transduction in the bacterial reaction centre. PhD thesis, University of Sheffield, United Kingdom, 1998.

[13] M.R. Jones, G.J.S. Fowler, L.C.D. Gibson, G.G. Grief, J.D. Olsen, W. Crielaard, C.N. Hunter, Construction of mutants of *Rhodobacter sphaeroides* lacking one or more pigment–protein complexes and complementation with reaction-centre, LH1, and LH2 genes, Mol. Microbiol. 6 (1992) 1173–1184.

[14] M.R. Jones, R.W. Visschers, R. Van Grondelle, C.N. Hunter, Construction and characterisation of a mutant of *Rhodobacter sphaeroides* with the reaction centre as the sole pigment–protein complex, Biochemistry 31 (1992) 4458–4465.

[15] M.R. Jones, M. Heer-Dawson, T.A. Mattioli, C.N. Hunter, B. Robert, Site-specific mutagenesis of the reaction centre from *Rhodobacter sphaeroides* studied by Fourier transform Raman spectroscopy: mutations at tyrosine M210 do not affect the electronic structure of the primary donor, FEBS Lett. 339 (1994) 18–24.

[16] K.E. McAuley-Hecht, P.K. Fyfe, J.P. Ridge, S.M. Prince, C.N. Hunter, N.W. Isaacs, R.J. Cogdell, M.R. Jones, Structural studies of wild type and mutant reaction centres from an antenna-deficient strain of *Rhodobacter sphaeroides*: monitoring the optical properties of the complex from cell to crystal, Biochemistry 37 (1998) 4740–4750.

[17] S.K. Buchanan, G. Fritzsch, U. Ermler, H. Michel, New crystal form of the photosynthetic reaction centre from *Rhodobacter sphaeroides* of improved diffraction quality, J. Mol. Biol. 230 (1993) 1311–1314.

[18] Z. Otwinowski, W. Minor, Processing of X-ray diffraction data collected in oscillation mode, Methods Enzymol. 276 (1997) 307–326.

[19] G.N. Murshudov, A.A. Vagin, E.J. Dodson, Refinement of macromolecular structures by the maximum-likelihood method, Acta Crystallogr., D Biol. Crystallogr. 53 (1997) 240–255.

[20] P.J. Kraulis, Molscript—a program to produce both detailed and schematic plots of protein structures, J. Appl. Crystallogr. 24 (1991) 946–950.

[21] E.A. Merritt, D.J. Bacon, Raster3D: photorealistic molecular graphics, Methods Enzymol. 277 (1997) 505–524.

[22] D.E. McRee, XtalView: a visual protein crystallographic software system for XII/Xview, J. Mol. Graph. 10 (1992) 44–46.

[23] M.Y. Okamura, M.A. Steiner, G. Feher, Characterisation of reaction centers from photosynthetic bacteria: I. Subunit structure of the pro-

tein mediating the primary photochemistry in *Rhodopseudomonas spheroides* R-26, Biochemistry 13 (1974) 1394–1402.
[24] P.K. Fyfe, J.P. Ridge, K.E. McAuley, R.J. Cogdell, N.W. Isaacs, M.R. Jones, Structural consequences of the replacement of glycine M203 by aspartic acid in the reaction centre from *Rhodobacter sphaeroides*, Biochemistry 39 (2000) 5953–5960.
[25] U. Ermler, G. Fritzsch, S.K. Buchanan, H. Michel, Structure of the photosynthetic reaction-center from *Rhodobacter sphaeroides* at 2.65-angstrom resolution—cofactors and protein–cofactor interactions, Structure 2 (1994) 925–936.
[26] U. Ermler, H. Michel, M. Schiffer, Structure and function of the photosynthetic reaction center from *Rhodobacter sphaeroides*, J. Bioenerg. Biomembranes 26 (1994) 5–15.
[27] J. Deisenhofer, O. Epp, I. Sinning, H. Michel, X-ray structure analysis of a membrane protein complex-electron-density map at 3 Å resolution and a model of the chromophores of the photosynthetic reaction center from *Rhodopseudomonas viridis*, J. Mol. Biol. 246 (1995) 429–457.
[28] M. Bonhivers, M. Desmadril, G.S. Moeck, P. Boulanger, A. Colomer-Pallas, L. Letellier, Stability studies of FhuA, a two-domain outer membrane protein from *Escherichia coli*, Biochemistry 40 (2001) 2606–2613.
[29] T. Haltia, E. Friere, Forces and factors that contribute to the structural stability of membrane-proteins, Biochim. Biophys. Acta 1228 (1995) 1–27.
[30] Y. Zhou, J.U. Bowie, Building a thermostable membrane protein, J. Biol. Chem. 275 (2000) 6975–6979.
[31] A.F. Boonstra, L. Germeroth, E. Boekema, Structure of the light-harvesting antenna from *Rhodospirillum molischianum* studied by electron microscopy, Biochim. Biophys. Acta 1184 (1994) 227–234.
[32] S. Karrasch, P.A. Bullough, R. Ghosh, The 8.5 Å projection map of the light-harvesting complex I from *Rhodospirillum rubrum* reveals a ring composed of 16 subunits, EMBO J. 14 (1995) 631–638.
[33] T. Walz, S.J. Jamieson, C.M. Bowers, P.A. Bullough, C.N. Hunter, Projection structures of three photosynthetic complexes from *Rhodobacter sphaeroides*: LH2 at 6 angstrom LH1 and RC-LH1 at 25 angstrom, J. Mol. Biol. 282 (1998) 833–845.
[34] H. Stahlberg, J. Dubochet, H. Vogel, R. Ghosh, Are the light-harvesting I complexes from *Rhodospirillum rubrum* arranged around the reaction centre in a square geometry?, J. Mol. Biol. 282 (1998) 819–831.
[35] C. Jungas, J.L. Ranck, J.L. Rigaud, P. Joliot, A. Vermeglio, Supramolecular organization of the photosynthetic apparatus of *Rhodobacter sphaeroides*, EMBO J. 18 (1999) 534–542.
[36] S.J. Jamieson, P.Y. Wang, P. Qian, J.Y. Kirkland, M.J. Conroy, C.N. Hunter, P.A. Bullough, Projection structure of the photosynthetic reaction centre–antenna complex of *Rhodospirillum rubrum* at 8.5 angstrom resolution, EMBO J. 21 (2002) 3927–3935.
[37] C.A. Yu, S.H. Gwak, L. Yu, Studies on protein–lipid interactions in cytochrome-*c* oxidase by differential scanning calorimetry, Biochim. Biophys. Acta 812 (1985) 656–664.
[38] A. Ortega, J. Santiago-García, J. Mas-Olivia, J.R. Lepock, Cholesterol increases the thermal stability of the Ca^{2+}/Mg^{2+}-ATPase of cardiac microsomes, Biochim. Biophys. Acta 1283 (1996) 45–50.
[39] L.R. Maneri, P.S. Low, Structural stability of the erythrocyte anion transporter, band-3, in different lipid environments—a differential scanning calorimetric study, J. Biol. Chem. 263 (1988) 16170–16178.
[40] T.W. Kahn, J.M. Sturtevant, D.M. Engelman, Thermodynamic measurements of the contributions of helix-connecting loops and of retinal to the stability of bacteriorhodopsin, Biochemistry 31 (1992) 8829–8839.
[41] G.B. Birrell, W.R. Sistrom, O.H. Griffith, Lipid–protein associations in chromatophores from the photosynthetic bacterium *Rhodopsuedomonas sphaeroides*, Biochemistry 17 (1978) 3768–3773.
[42] W. Welte, W. Kreutz, Formation, structure and composition of a planar hexagonal lattice composed of specific protein–lipid complexes in the thylakoid membranes of *Rhodopseudomonas viridis*, Biochim. Biophys. Acta 692 (1982) 479–488.
[43] P.V. Ioannou, B.T. Golding, Cardiolipins: their chemistry and biochemistry, Prog. Lipid Res. 17 (1979) 279–318.
[44] F.L. Hoch, Cardiolipins and biomembrane function, Biochim. Biophys. Acta 1113 (1992) 71–133.
[45] G. Fritzsch, L. Kampmann, G. Kapaun, H. Michel, Water clusters in the reaction centre of *Rhodobacter sphaeroides*, Photosynth. Res. 55 (1998) 127–132.
[46] E.C. Abresch, M.L. Paddock, M.H.B. Stowell, T.M. McPhillips, H.L. Axelrod, S.M. Soltis, D.C. Rees, M.Y. Okamura, G. Feher, Identification of proton transfer pathways in the X-ray crystal structure of the bacterial reaction center from *Rhodobacter sphaeroides*, Photosynth. Res. 55 (1998) 119–125.
[47] C.R.D. Lancaster, H. Michel, B. Honig, M.R. Gunner, Calculated coupling of electron and proton transfer in the photosynthetic reaction center of *Rhodopseudomonas viridis*, Biophys. J. 70 (1996) 2469–2492.
[48] T.A. Wells, E. Takahashi, C.A. Wraight, Primary quinone (Q_A) binding site of bacterial photosynthetic reaction centers: mutations at residue M265 probed by FTIR spectroscopy, Biochemistry 42 (2003) 4064–4074.
[49] L. Rinyu, E.W. Martin, E. Takahashi, P. Maróti, C.A. Wraight, Modulation of the free energy of the primary quinone acceptor (Q_A) in reaction centers from *Rhodobacter sphaeroides*: contributions from the protein and protein–lipid(cardiolipin) interactions, Biochim. Biophys. Acta,(in press).
[50] G. Katona, U. Andreasson, E.M. Landau, L.E. Andreasson, R. Neutze, Lipidic cubic phase crystal structure of the photosynthetic reaction centre from *Rhodobacter sphaeroides* at 2.35 angstrom resolution, J. Mol. Biol. 331 (2003) 681–692.
[51] F.W. Lau, J.U. Bowie, A method for assessing the stability of a membrane protein, Biochemistry 36 (1997) 5884–5892.
[52] A.T. Brünger, Free R-value—a novel statistical quantity for assessing the accuracy of crystal-structures, Nature 335 (1992) 472–475.
[53] R.A. Laskowski, W.W. MacArthur, D.S. Moss, J.M. Thornton, PROCHECK—a program to check the stereochemical quality of protein structures, J. Appl. Crystallogr. 26 (1993) 283–291.
[54] D.W.J. Cruickshank, Remarks about protein structure precision, Acta Crystallogr., D Biol. Crystallogr. 55 (1999) 583–601.